Supplementary Information

Characterization of a Liquid-Core Waveguide cell for studying the chemistry of light-induced degradation

Iris Groeneveld[a], Suzan E. Schoemaker[a], Govert W. Somsen[a], Freek Ariese[b], Maarten R. van Bommel[c,d]

[a] *Division of Bioanalytical Chemistry, Amsterdam Institute for Molecular and Life Sciences, Vrije Universiteit Amsterdam, De Boelelaan 1108, 1081 HZ Amsterdam, The Netherlands, i.groeneveld@vu.nl, +31 (0) 20 59 86 892;*

[b] *LaserLaB, Vrije Universiteit Amsterdam, The Netherlands;*

[c] *Analytical Chemistry Group, van 't Hoff Institute for Molecular Sciences, University of Amsterdam, Science Park 904, 1098 XH Amsterdam, The Netherlands;*

[d] *Conservation and Restoration of Cultural Heritage, Amsterdam School for Heritage, Memory and Material Culture, University of Amsterdam, P.O. Box 94552, 1091 GN, Amsterdam, The Netherlands.*

A. Schematic drawing coupling pieces

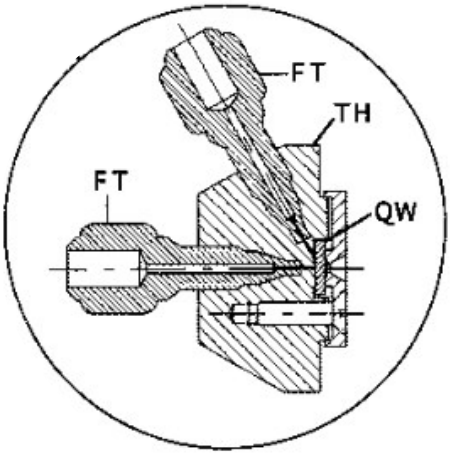

Figure A.1: Cross section drawing of the coupling pieces of the LID (obtained from Dijkstra et al. [1]). FT: fingertight; TH: termination head; QW: quartz window.

B. Variation due to filling procedure

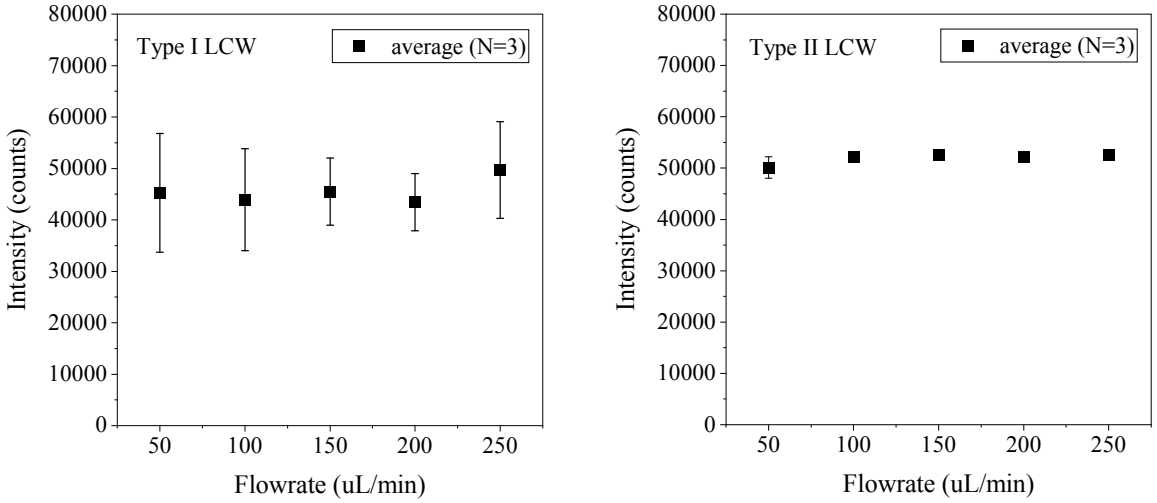

Figure B.1: Average transmitted light intensities (N=3) measured during the filling of a type I and type II LCW at different flow rates (50, 100, 150, 200, and 250 µL/min). The fluctuations in intensity in the type I LCW may be caused by the porous wall since these fluctuations are not present in the non-porous type II LCW.

C. Photon flux by actinometry

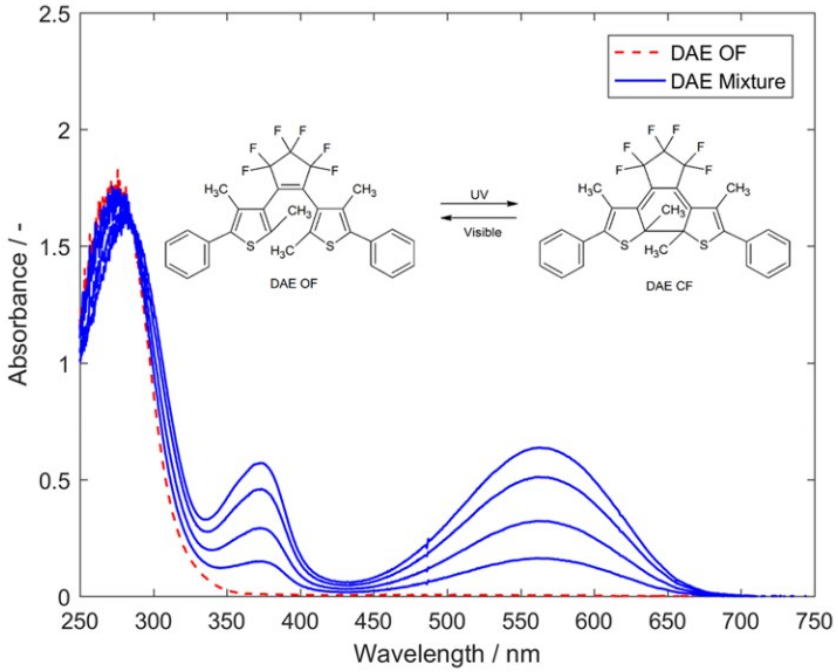

Figure C.1: The change in absorbance of DAE upon exposure of Vis or UV light (obtained from Roibu et al. [2]).

For the purpose of turning DAE-c into DAE-o, the lamp was turned off and the UV shortpass filter was replaced by the 578 nm bandpass filter. To start the ring-opening reaction, the lamp was turned on again and the absorption spectra of this process were recorded in real-time.

The speed at which DAE-c turns into DAE-o was used to calculate the photon flux. To do so, the molar absorption coefficient (ε) at 578 nm was calculated first. Using UV light, a solution of DAE was turned into DAE-c until the signal became stable, indicating maximum conversion from open to closed, which is estimated to be about 79%, according to Irie et al. [3]. Then, to calculate the concentration of DAE-c at maximum conversion, the ε at 562 nm was obtained from Sumi et al. [4]. With an ε of 10900 $M^{-1}cm^{-1}$ at 562 nm, we determined the concentration of DAE-c to be $7.8*10^{-6}$ M. Using this concentration, the ε_{578nm} was also determined from the absorption spectrum at maximum conversion, which was 9954 $M^{-1}cm^{-1}$.

Another important note has to be made regarding the solvent. We observed that if the Teflon material of the LCW was exposed to hexane for too long, the LCW started to deform. As the hexane is partially absorbed by the Teflon, the material swells over time. This does not have to cause a direct problem, except when the LCW starts to touch the outer tubing. A bright spot was observed at the location where this happened, indicating light loss. Therefore, the LID cell had to be filled with water for storage and in between experiments that were not performed consequently, which also made the tubing regain its original form.

Calculations:

The UV-induced conversion from the open to the closed form has a high quantum yield (0.45 at λ = 268 nm according to Sumi et al. [4]), whereas the conversion back to the open form has a very low quantum yield which is wavelength dependent. Sumi et al. report the following dependence for the opening reaction [4]:

$$\log \Phi_{CO} = -2.67 + \frac{526}{\lambda},\ 480\ nm \leq \lambda \leq 620\ nm \qquad \text{(Eq. C.1)}$$

in which Φ_{CO} is the quantum yield for the opening reaction and λ is the wavelength of irradiation (nm).

The calculation of the photon flux based on actinometric experiments is, traditionally, done as described in this section [2,5–7]. Consider a photo-induced reaction of compound X to compound Y, this can schematically be written as:

$$X \overset{light}{\rightarrow} Y$$

In such reactions, the absorption of an incoming photon is linked to the conversion (*R*) of X into Y. This can be visualized by, for example, the appearance of a new peak in the absorbance spectrum that is characteristic for the product formed. Actinometry experiments are set-up to track this change in concentration using absorption measurements. In the case of

the commonly used ferrioxalate actinometer, the conversion (*R*) is determined by means of a calibration curve.

The quantum yield, ϕ_λ , represents the efficiency of a photo-induced reaction. It provides information about the number of the absorbed photons accompanied for such a reaction. Therefore, the change in concentration, *c*, of the compound X can be calculated by:

$$\frac{dc}{dt} = -\phi_\lambda \frac{I_{abs}}{V_r} \quad \text{(Eq. C.2)}$$

in which I_{abs} is the absorbed photon flux in Einstein s^{-1} and V_r is the reaction volume (L). However, no complete absorption is achieved, so, Lambert-Beer is needed:

$$A = -log\frac{I_{transmitted}}{q_\lambda} = \varepsilon c l \quad \text{(Eq. C.3)}$$

in which *A* is the absorbance; I_{trans} is the transmitted light, q_λ is the initial (overall) photon flux (both einstein s^{-1}); ε is the absorption coefficient ($M^{-1}cm^{-1}$); and l is the optical pathlength (cm). Thereby, making:

$$I_{abs} = q_\lambda(1 - 10^{-\varepsilon c l}) \quad \text{(Eq. C.4)}$$

Substitution of equation C.4 into equation C.2 results in [2]:

$$\frac{dc}{dt} = -\frac{\phi_\lambda q_\lambda}{V_r}(1 - 10^{-\varepsilon c l}) \quad \text{(Eq. C.5)}$$

Integration of the formula gives a formula that relates the conversion to the photon flux:

$$\left(\phi_\lambda \frac{q_\lambda}{V}\right)t = c(0)R + \frac{1}{\varepsilon l} ln(\frac{1 - 10^{-\varepsilon c(0) l}}{1 - 10^{-\varepsilon c(t) l}}) \quad \text{(Eq. C.6)}$$

in which *t* is the time of irradiation (s), *R* is the conversion of compound X to Y, *c(0)* is the initial concentration (M), *c(t)* is the concentration at time *t*.

However, in our system, online and direct detection is required, since the exact number of photons inside the LCW must be determined. Lehóczki et al. proposed an alternative way of actinometry with online spectrophotometric detection [8]. They avoided the need of a calibration of the light source by continuously monitoring the absorption over time. A specific wavelength was chosen of which the change in absorbance was directly used to calculate the photon flux. They proposed the following formula, which was used in our calculations of the photon flux:

$$q_\lambda = \left(\frac{dA_\lambda}{dt}\right) * \frac{V_r}{\phi_\lambda \varepsilon_\lambda l} \qquad \text{(Eq. C.7)}$$

in which q_λ is the overall photon flux (einstein s^{-1}); V_r the reaction volume (L); ϕ_λ the quantum yield at wavelength λ; ε is the absorption coefficient ($M^{-1}cm^{-1}$) and l is the optical pathlength (= length of the LCW, cm).

D. CV and EY degradation

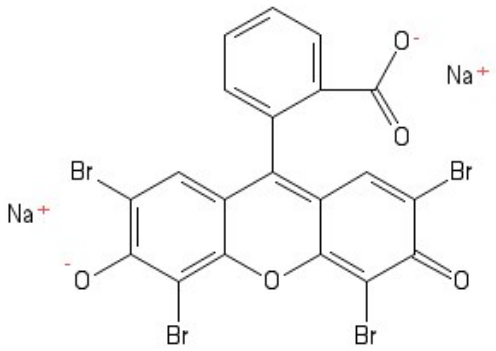

Figure D.1: Molecular structure of eosin Y.

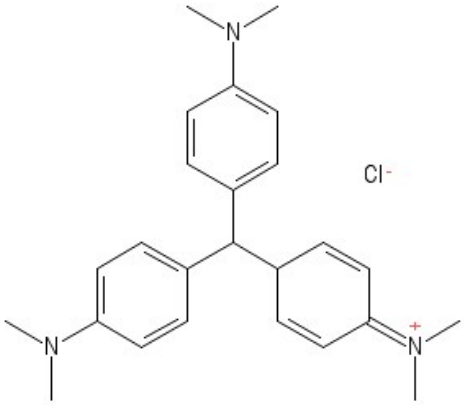

Figure D.2: Molecular structure of crystal violet.

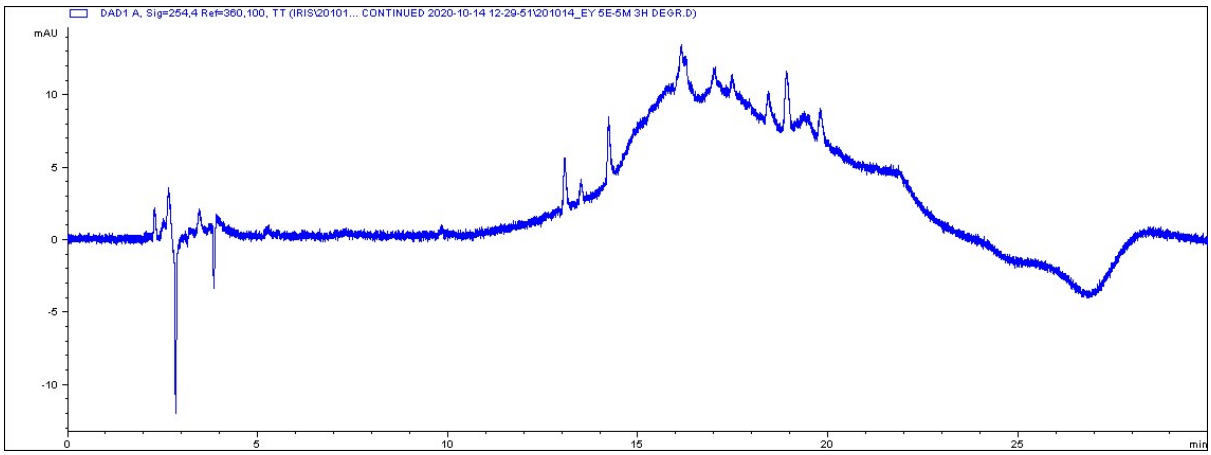

Figure D.3: LC-PDA chromatogram obtained of analysis of an EY solution after 3-hr exposure, extracted at 254 nm.

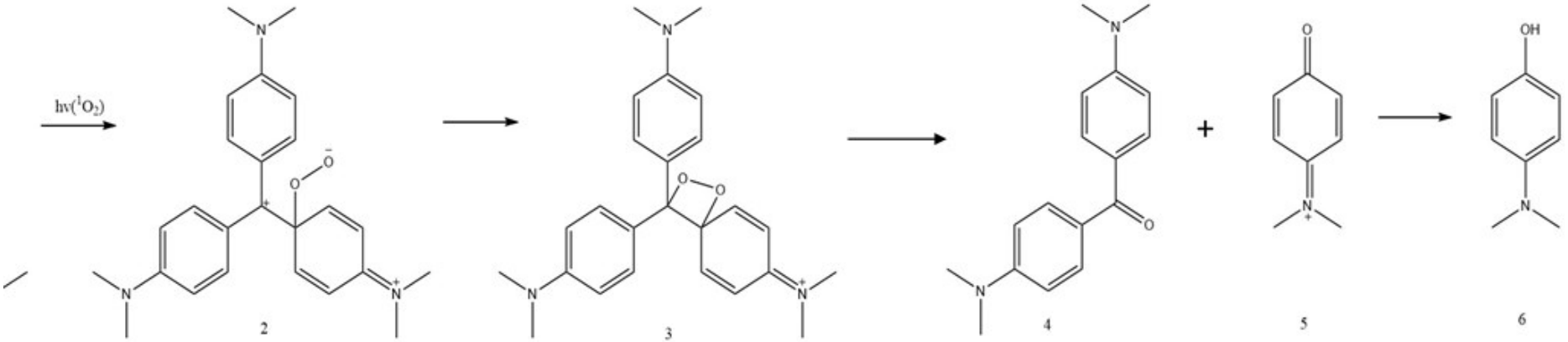

Figure D.4: Proposed reaction mechanism for photodegradation of crystal violet. Both demethylation (1 → 7) takes place, as well as cleavage of the central carbon-atom, resulting in Michler's ketone (4) and dimethylaminophenol (6). Figure obtained from Confortin and Kuramoto [9,10].

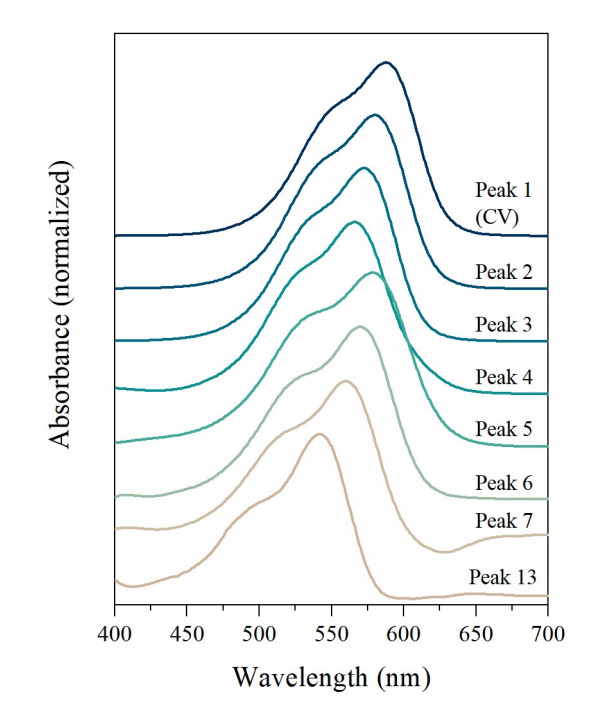

Figure D.5: Normalized and smoothed absorption spectra of CV (peak 1) and degradation products (peaks 2-7 and 13) obtained from LC-PDA analysis of the 5-hr exposed CV sample.

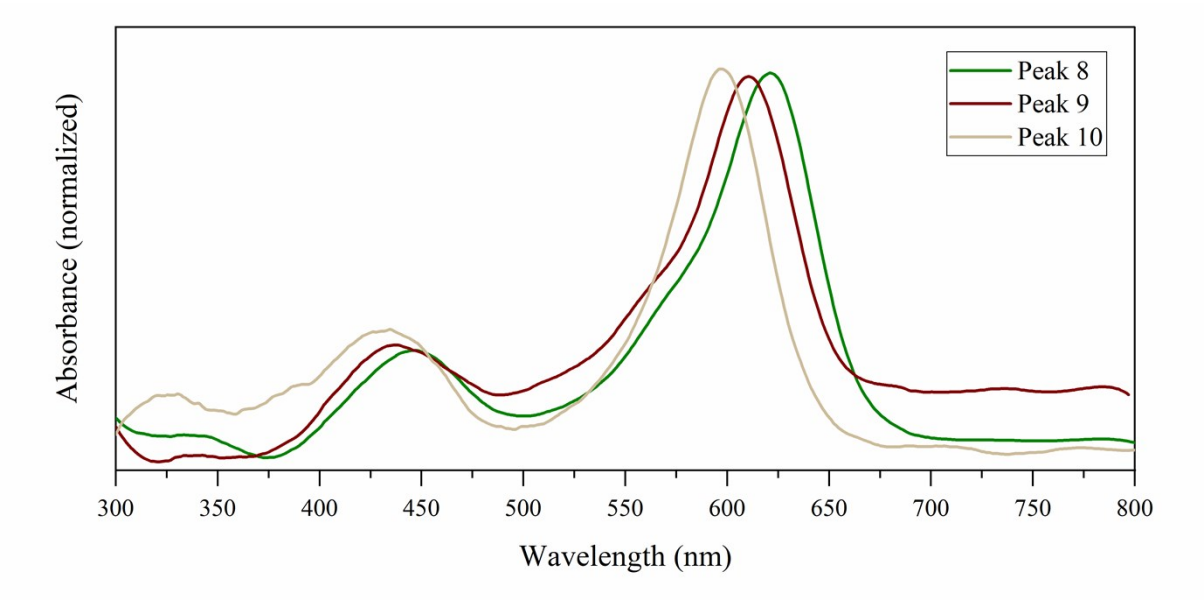

Figure D.6: Normalized and smoothed absorption spectra of peaks 8 – 10 obtained during LC-PDA analysis of the 5-hr exposed CV sample.

Table D.1: LC-PDA peak table of the 5-hr exposed CV sample with tentative assignments.

Peak number	RT (min)	abs max (nm)	Tentative assignment
1	18.99	590	CV
2	18.67	582	mono-demethylated CV
3	18.30	574	bis-demethylated CV
4	17.89	568	tri-demethylated CV
5	17.79	580	isomer of peak 4
6	17.43	571	tetra-demethylated CV
7	17.01	560	penta-demethylated CV
8	16.58	620	diamond green equivalent
9	16.50	610	diamond green equivalent
10	16.30	600	diamond green equivalent
11	16.13	250-350	-
12	15.74	250-350	-
13	15.00	546	pararosaniline
14	13.56	250-350	-

References

1 R. J. Dijkstra, A. N. Bader, G. P. Hoornweg, U. A. T. Brinkman and C. Gooijer, *Anal. Chem.*, 1999, **71**, 4575–4579.

2 A. Roibu, S. Fransen, M. E. Leblebici, G. Meir, T. Van Gerven and S. Kuhn, *Sci. Rep.*, 2018, **8**, 1–10.

3 M. Irie, K. Sakemura, M. Okinaka and K. Uchida, *J. Org. Chem.*, 1995, **60**, 8305–8309.

4 T. Sumi, Y. Takagi, A. Yagi, M. Morimoto and M. Irie, *Chem. Commun.*, 2014, **50**, 3928–3930.

5 E. Stadler, A. Eibel, D. Fast, H. Freißmuth, C. Holly, M. Wiech, N. Moszner and G. Gescheidt, *Cite this Photochem. Photobiol. Sci*, 2018, **17**, 660.

6 T. Aillet, K. Loubiere, O. Dechy-Cabaret, L. E. Prat and L. Prat, *Int. J. Chem. React. Eng.*, 2014, **12**, 1–13.

7 K. L. Willett and R. A. Hites, *Lab. 900 J. Chem. Educ.* •, , DOI:10.1021/ed077p900.

8 T. Lehóczki, É. Józsa and K. Osz, *J. Photochem. Photobiol. A Chem.*, 2013, **251**, 63–68.

9 D. Confortin, H. Neevel, M. Brustolon, L. Franco, A. J. Kettelarij, R. M. Williams and M. R. Van Bommel, *J. Phys. Conf. Ser.*, 2010, **231**, 1–9.

10 N. Kuramoto and T. Kitao, *Dye. Pigment.*, 1982, **3**, 49–58.